第23卷 第6期 原子与分子物理学报 Vol.23 No.6
2006年12月 JOURNAL OF ATOMIC AND MOLECULAR PHYSICS Dec. 2006

文章编号：1000-0364(2006)06-0981-09

# HNO二聚体蓝移氢键的理论研究*

刘 颖[1,2**]，刘文清[1]，李海洋[1,3]，杨 颙[1,2]，程 爽[1,2]

(1. 中国科学院安徽光学精密机械研究所环境光学与技术重点实验室，合肥 230031；
2. 中国科学院研究生院，北京 100039；3. 中国科学院大连化学物理研究所，大连 116023)

**摘 要**：利用分子轨道从头算理论和密度泛函理论结合不同理论基组对于N－H…O蓝移氢键进行了详细的研究.利用标准方法和均衡校正方法对二聚体进行了几何优化，振动频率和相互作用能的计算.拓扑学和自然键轨道理论对于蓝移氢键的本质进行分析.自然键轨道(NBO)分析表明，$\sigma^*$(N－H)轨道上电子密度降低是电子密度重排效应的结果.分子内电子重排、轨道再杂化和电子受体内部结构重组共同作用结果导致了N－H的振动频率大幅蓝移现象的出现.

**关键词**：蓝移氢键；原子在分子中拓扑学分析；自然键轨道分析；电子密度重排效应；结构重组

**中图分类号**：O643 **文献标识码**：A

# Theoretical study of hydrogen bond blue-shift in the HNO dimer

LIU Ying[1,2], LIU Wen-qing[1], LI Hai-yang[1,3], YANG Yong[1,2], CHENG Shuang[1,2]

(1. Key Laboratory of Environmental Optical and Technology, Anhui Institute of Optics and Fine Mechanics, Chinese Academy of Sciences, Hefei 230031, P. R. China;
2. Graduate School of Chinese Academy of Sciences, Beijing 100039, P. R. China;
3. Dalian Institute of Chemical Physics, Chinese Academy of Sciences, Dalian 116023, P. R. China)

**Abstract**: *Ab initio* molecular orbital and density functional theory (DFT) in conjunction with different basis sets calculations were performed to study the N－H…O blue-shifted hydrogen bond in the HNO dimer. The geometric structures, vibrational frequencies and interaction energies were calculated by both standard and CP-corrected methods. The topological and NBO analysis were investigated the origin of N－H bond blue shift. From the NBO analysis, the decrease in the $\sigma^*$(N－H) is due to the significant electron density redistribution effect. The electron density redistribution effect, rehybridizative effect and the structure re-organization are contributed to the large blue shift of the N－H stretching frequency.

**Key words**: Blue-shifted hydrogen bond, atoms in molecules topological analysis, natural bond orbital analysis, electron density redistribution, structure reorganization

## 1 Introduction

Hydrogen bonding is an important concept in chemistry. The investigation of the hydrogen bonding has attracted considerable attention over the years. Most hydrogen bonds are of X－H…Y type, where X is an electronegative atom and Y is either

* 收稿日期：2005-12-29
基金项目：中国科学院合肥物质科学研究院计算中心支持项目(0330405002)
作者简介：刘颖(1978－)，女，辽宁朝阳人，博士研究生，主要研究方向为原子与分子物理化学的理论研究.
** 通讯作者：E-mail: lying@aiofm.ac.cn

an electronegative atom having one or more lone electron pairs or a region of excess electron density like aromatic $\pi$-system[1,2]. Recently, a new type of intermolecular bonding, termed blue-shifting hydrogen bond that is accompanied by X－H bond contraction and a blue shift of the X－H bond stretching frequency continues to receive significant experimental and theoretical attention[3~11]. The blue-shifted H-bonds that have been studied so far are mainly C－H⋯Y systems. To rationalize the C－H bond shortening and the consequent blue shift of the C－H stretching frequency, two explanations have been proposed[12]. N atom is more electronegative than C atom and N－H bond is a better proton donor than C－H bond, the phenomenon of N－H⋯Y blue-shifted H-bonds are very interesting. Both Hobza and Li *et al* have predicted a blue-shifted or improper N－H⋯F H-bond existing in the $NHF_2$⋯HF complex at the MP2/6-31G($d$, $p$) and MP2/6-311＋G($d$, $p$), respectively[13,14]. Unexpectedly, Lu *et al* has predicted a red-shifted for normal N－H⋯F H－bond in this complex at the B3LYP/6-31＋G($d$, $p$), B3LYP/6-311＋G($d$, $p$) and B3LYP/6-311＋＋G(3$df$,3$pd$) levels, respectively[15]. Both MP2 and B3LYP computations have their own supporting instances from the point of agreement between theoretical prediction and experimental measurement[3,10]. Consequently, it is difficult to decide which H-bond type the N－H⋯F is from the point of theory in the $NHF_2$⋯HF complex. To the best of our knowledge, the researches on N－H⋯O hydrogen bond systems are scant.

HNO is important in the processes such as pollution formation, energy release in propellants and fuel combustion[16]. Many theoretical and experimental studies were performed. HNO dimer involving in important HNO self-combustion reaction was paid attention. Ruud *et al* used MP2/6-31G($d$, $p$) and MP4/6-311＋G(2$df$,2$pd$) to study the HNO dimerization and decomposition processes[17]. Peters has studied the hydrogen bond formation in HNO dimer at MP2 in conjunction with 6-31＋G** level, obtaining its optimized geometries and vibrational frequencies[18]. However, up to now, there are no post Hartree-Fock and density functional theory (DFT) calculations at large basis set levels such as 6-311＋G(3$df$,2$p$) or 6-311＋＋G(3$df$,3$pd$) and the CP corrected optimized structures, vibrational frequencies and interaction energies of this dimer in the literature. Moreover, the origin of the N－H blue shift was not given. In this paper, we performed *ab initio* molecular orbital and density functional theory in conjunction with different basis sets calculations (both standard and CP calculations) to report the structure of the HNO dimer, interaction energies and vibrational frequencies. We confirm the existence of N－H truly blue shift, then, it is well explained what lead to the large blue-shifted of the N－H vibrational frequencies. This work will be much helpful to understand the nature of N-H blue-shifted hydrogen bond deeply.

## 2 Computational methods

The HNO dimer was investigated by different theoretical methods including Hartree-Fock (HF), density functional theory (DFT) (Becke's three parameter hybrid functional in conjunction with Lee, Yang, and Parr's correlation functional, abbreviated as B3LYP), and second-order Møller-Plesset perturbation (MP2) methods (Hartree-Fock calculation followed by Møller-Plesset correlation energy correction truncated at second order) in conjunction with different basis sets. Both standard and counterpoise-corrected gradient optimization were performed and followed by vibrational frequency calculation to confirm the actual minima obtained. And the interaction energies were calculated at the same theoretical levels. The basis set superposition errors (BSSE) were calculated according to the counterpoise method proposed by Boys and Bernardi[19]. Natural bond orbital (NBO) and atoms in molecules (AIM) analyzes were performed at the MP2/6-311＋＋G(3$df$, 3$pd$) level[20,21]. All calculations were carried out using the Gaussian03 package[22].

# 3 Results and discussion

## 3.1 Geometries, frequencies and interaction energies

Table 1 Characteristics of HNO dimer at HF, B3LYP and MP2 level in conjunction with different basis sets

| | 6-31G* | 6-311G** | 6-311+G** | aug-cc-pvdz | 6-311+G(3*df*,2*p*) | 6-311++G(3*df*,3*pd*) |
|---|---|---|---|---|---|---|
| | | | HF | | | |
| *r*(O4…H1)/nm | 0.24249 | 0.24470 | 0.24947 | 0.24980 | 0.25087 | 0.25087 |
| *r*CP(O4…H1)/nm | 0.24872 | 0.24848 | 0.25113 | 0.25218 | 0.25337 | 0.25337 |
| *r*(O3…H6)/nm | 0.24364 | 0.24468 | 0.24958 | 0.25036 | 0.25134 | 0.25134 |
| *r*CP(O3…H6)/nm | 0.24928 | 0.24900 | 0.25123 | 0.25245 | 0.25339 | 0.25339 |
| Δ*r*(N2－H1)/nm | －0.00048 | －0.00040 | －0.00032 | －0.00031 | －0.00030 | －0.00030 |
| Δ*r*CP(N2－H1)/nm | －0.00036 | －0.00037 | －0.00028 | －0.00029 | －0.00029 | －0.00028 |
| Δ*r*(N5－H6)/nm | －0.00048 | －0.0004 | －0.00032 | －0.00031 | －0.00030 | －0.00030 |
| Δ*r*CP(N5－H6)/nm | －0.00035 | －0.00036 | －0.00028 | －0.00029 | －0.00029 | －0.00028 |
| $\Delta v_1/cm^{-1}$ | 94 | 83 | 68 | 66 | 67 | 68 |
| $\Delta v_1CP/cm^{-1}$ | 74 | 75 | 62 | 63 | 63 | 62 |
| $\Delta v_2/cm^{-1}$ | 90 | 79 | 65 | 62 | 63 | 64 |
| $\Delta v_2CP/cm^{-1}$ | 70 | 71 | 59 | 59 | 60 | 59 |
| | | | B3LYP | | | |
| *r*(O4…H1)/nm | 0.22962 | 0.23107 | 0.23842 | 0.24059 | 0.23923 | 0.23923 |
| *r*CP(O4…H1)/nm | 0.23816 | 0.23876 | 0.23982 | 0.24159 | 0.24184 | 0.24184 |
| *r*(O3…H6)/nm | 0.22907 | 0.23160 | 0.23838 | 0.24121 | 0.23923 | 0.23923 |
| *r*CP(O3…H6)/nm | 0.23828 | 0.23873 | 0.23982 | 0.24158 | 0.24182 | 0.24182 |
| Δ*r*(N2－H1)/nm | －0.00101 | －0.00086 | －0.00053 | －0.00057 | －0.00055 | －0.00054 |
| Δ*r*CP(N2－H1)/nm | －0.00083 | －0.00070 | －0.00052 | －0.00055 | －0.00049 | －0.00048 |
| Δ*r*(N5－H6)/nm | －0.00100 | －0.00086 | －0.00053 | －0.00057 | －0.00055 | －0.00054 |
| Δ*r*CP(N5－H6)/nm | －0.00083 | －0.00070 | －0.00052 | －0.00055 | －0.00049 | －0.00048 |
| $\Delta v_1/cm^{-1}$ | 161 | 149 | 98 | 101 | 99 | 99 |
| $\Delta v_1CP/cm^{-1}$ | 130 | 119 | 97 | 97 | 91 | 90 |
| $\Delta v_2/cm^{-1}$ | 146 | 134 | 89 | 90 | 89 | 89 |
| $\Delta v_2CP/cm^{-1}$ | 118 | 107 | 88 | 87 | 81 | 80 |
| | | | MP2 | | | |
| *r*(O4…H1)/nm | 0.23179 | 0.23598 | 0.24075 | 0.23523 | 0.23367 | 0.23458 |
| *r*CP(O4…H1)/nm | 0.24470 | 0.24660 | 0.24930 | 0.24051 | 0.23937 | 0.23925 |
| *r*(O3…H6)/nm | 0.23121 | 0.23576 | 0.24120 | 0.23504 | 0.23367 | 0.23457 |
| *r*CP(O3…H6)/nm | 0.24469 | 0.24660 | 0.24930 | 0.24048 | 0.23937 | 0.23925 |
| Δ*r*(N2－H1)/nm | －0.00074 | －0.00056 | －0.00044 | －0.00043 | －0.00044 | －0.00043 |
| Δ*r*CP(N2－H1)/nm | －0.00054 | －0.00044 | －0.00036 | －0.00041 | －0.00037 | －0.00039 |
| Δ*r*(N5－H6)/nm | －0.00074 | －0.00056 | －0.00044 | －0.00043 | －0.00044 | －0.00043 |
| Δ*r*CP(N5－H6)/nm | －0.00054 | －0.00044 | －0.00036 | －0.00041 | －0.00037 | －0.00039 |
| $\Delta v_1/cm^{-1}$ | 132 | 112 | 86 | 89 | 88 | 90 |
| $\Delta v_1CP/cm^{-1}$ | 98 | 88 | 73 | 84 | 78 | 80 |
| $\Delta v_2/cm^{-1}$ | 123 | 104 | 80 | 80 | 80 | 82 |
| $\Delta v_2CP/cm^{-1}$ | 91 | 81 | 68 | 76 | 71 | 73 |

$\Delta v_1$: The differences of N1－H2, N5－H6 symmetric stretch between the dimer and monomer;

$\Delta v_2$: The differences of N1－H2, N5－H6 asymmetric stretch between the dimer and monomer

Table 2 Interaction energies (in kcal/mol) of HNO dimer

| | HF /6-311++G (3*df*,3*pd*) | B3LYP /6-311++G (3*df*,3*pd*) | MP2 /6-311++G (3*df*,3*pd*) |
|---|---|---|---|
| $\Delta E_{standard}$ | -1.34 | -1.38 | -1.15 |
| $\Delta E_{CP}$ | -1.07 | -1.16 | -0.56 |

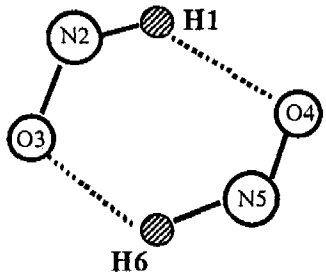


Fig.1 The optimized structure for the HNO dimer at MP2/6-311++G(3*df*,3*pd*) leved

Peters founded the two stable structure for the HNO dimer at MP2 in conjunction with 6-31+G** level. With hydrogen atoms on monomer and at least two proton acceptance sites, a feature to the dimer structures is a ring arrangement of six or five atoms using the MP2/6-31+G**[18]. However, in our work, for the five-membered structure, one imaginary vibrational frequency was found at the B3LYP level in conjunction with different basis sets and MP2 in conjunction with 6-311+G**, 6-311++G** level and will not be discussed hereafter. The characteristics of the HNO dimer determined by both standard and counterpoise-corrected (CP) optimization and the stretching frequency changes between the HNO dimer and monomer HNO are presented in Table 1 and Fig. 1. The structures and vibrational frequencies were calculated by both MP2, B3LYP and HF methods with the 6-31G*, 6-311G**, 6-311+G**, aug-cc-pvdz, 6-311+G(3*df*,2*p*) and 6-311++G(3*df*,3*pd*) basis sets, respectively. From Table 1, all bond distances obtained by the HF method are longer than those obtained by the DFT and MP2 methods. The results obtained by the MP2 method are in agreement with those by the DFT method. Recently, Hobza *et al* have pointed out the necessity of using the CP-corrected gradient optimization for the hydrogen bonds blue shift researches[23]. We performed the CP-corrected calculations for structure optimization, vibrational frequencies and interaction energies. All the corrected bond distances are longer than uncorrected ones.

From stretching frequency changes between the HNO dimer and the monomer HNO shown in Table 1, as far as the H-bond type prediction is concerned, the MP2 computation results are in agreement with those of the B3LYP but lower than those of HF. All indicate that the N2－H1 and N5－H6 stretching frequencies have very large blue shifts in the HNO dimer. The CP-corrected gradient optimization will affect not only the interaction energy but also the geometry and stretching frequency of the X－H···Y H-bond. However, the large blue shift of the N2－H1 and N5－H6 stretching frequency in the HNO dimer by HF, B3LYP and MP2 calculation still exists, as shown in Table 1, in spite of application of the CP-corrected. On the other hand, the blue shift of the N2－H1 and N5－H6 stretching frequency by CP-corrected optimization is slightly smaller but still in reasonable agreement with these of the N2－H1 and N5－H6 stretching frequency by standard optimization. On the basis of these analyses, we can confirm that the N2－H1 and N5－H6 stretching frequencies both display very large blue shifts.

As shown in Table 2, the intermolecular interaction energies with both BSSE correction and ZPVE correction are in reasonable agreement at various levels in conjunction with 6-311++G(3*df*,3*pd*) basis set. The standard interaction energies for the HNO dimer is －1.34, －1.38, －1.15 kcal/mol obtained at HF/6-311++G(3*df*,3*pd*), B3LYP/6-311++G(3*df*,3*pd*) and MP2/6-311++G(3*df*,3*pd*), respectively. The BSSE correction and ZPVE correction are important to accurately describe the intermolecular interaction energies. And the CP-corrected interaction energies for the HNO dimer is －1.07, －1.16 and －0.56 kcal/mol at HF/6-311++G(3*df*,3*pd*), B3LYP/6-311++G(3*df*,3*pd*) and MP2/6-311++G(3*df*,3*pd*), respectively.

### 3.2 AIM analysis

The rigorous AIM theory has been success fully applied in characterizing hydrogen bonds of different

strengths in a wide variety of molecular complexes[24, 25]. Popelier proposed a set of criteria for the existence of H bonding within the AIM formalism[26]. The most prominent evidence of hydrogen bonding is the existence of a bond path between the donor hydrogen nucleus and the acceptor, containing a bond critical point (BCP) at which the electron density ($\rho$) ranges from 0.002 to 0.035 a. u. and the Laplacian of the electron density ($\nabla^2\rho$) ranges from 0.024 to 0.139 a. u.. According to the topological analysis of electron density in the theory of AIM, $\rho$ is used to describe the strength of a bond. The electron density ($\nabla^2\rho$) is used to characterize the bond. Where $\nabla^2\rho < 0$, the bond is covalent bond, as $\nabla^2\rho > 0$, the bond belongs to the ionic bond, hydrogen bond or van der Waals interaction.

As shown in Table 3, the values of the electron density $\rho$ for O4···H1 and O3···H6 in the HNO dimer are 0.011326 and 0.011326 a. u., respectively, which of the $\nabla^2\rho$ for O4···H1 and O3···H6 are 0.04209 and 0.04209 a. u., respectively. These values do fall within the proposed typical range of the H-bonds. On the basis of the AIM topological analysis, we have proved that the N2 − H1···O4 and N5 − H6···O3 bonds can be classified as H-bonds in the HNO dimer. It should be pointed out that the N2 − H1 and N5 − H6 bonds both exhibit a large blue shift. However, the AIM analysis does not reveal the origin of the blue-shifted H-bonds. This problem was solved by performing the natural bond orbital (NBO) analysis.

Table 3 Topological parameters of the bond critical point at the MP2/6-311 + + G(3*df*,3*pd*) level

| BCP | $\rho$ | $\nabla^2\rho$ | $\lambda_1$ | $\lambda_2$ | $\lambda_3$ |
|---|---|---|---|---|---|
| O4···H1 | 0.011326 | 0.04209 | −0.01232 | −0.01232 | 0.06672 |
| O3···H6 | 0.011326 | 0.04209 | −0.01232 | −0.01232 | 0.06672 |

Table 4 NBO analysis of the HNO and HNO dimer at the MP2/6-311 + + G(3*df*,3*pd*) level

| | HNO | HNO dimer |
|---|---|---|
| $E^{(2)}n_1(O4)\rightarrow\sigma^*(N2-H1)$/kcal mol$^{-1}$ | – | 0.55 |
| $E^{(2)}n_2(O4)\rightarrow\sigma^*(N2-H1)$/kcal mol$^{-1}$ | – | 0.85 |
| $E^{(2)}n_1(O3)\rightarrow\sigma^*(N5-H6)$/kcal mol$^{-1}$ | – | 0.55 |
| $E^{(2)}n_2(O3)\rightarrow\sigma^*(N5-H6)$/kcal mol$^{-1}$ | – | 0.85 |
| $E^{(2)}n_2(O3)\rightarrow\sigma^*(N2-H1)$/kcal mol$^{-1}$ | 18.52 | 15.88 |
| $E^{(2)}n_1(O4)\rightarrow\sigma^*(N5-H6)$/kcal mol$^{-1}$ | – | 15.88 |
| $\sigma^*(N2-H1)$/e | 0.03013 | 0.02789 |
| $\sigma^*(N5-H6)$/e | – | 0.02789 |
| $q$(H1)/e | 0.25897 | 0.28793 |
| $q$(H6)/e | | 0.28793 |
| $R_E(N2-H1)$ | | 0.5303 |
| $R_E(N5-H6)$ | | 0.5303 |
| spn(N2 − H1) | sp4.03 | sp3.79 |
| % s-char | 19.79% | 20.78% |
| pol N2% | 63.99% | 65.36% |
| ($\sigma_{N2-H1}$), H1% | 36.01% | 34.64% |
| spn(N5 − H6) | – | sp3.79 |
| % s-char | – | 20.78% |
| pol N5% | – | 65.36% |
| ($\sigma_{N5-H6}$), H6% | | 34.64% |

### 3.3 NBO analysis

For a better understanding of the origin of the blue-shifted hydrogen bonds, natural bond orbital (NBO) analysis has been carried out at the MP2/6-311++G(3df,3pd) level and the corresponding results are collected in Table 4. Recently, Alabugin *et al* showed that structural reorganization of X－H bond in the process of both blue-shifted and red-shifted H-bonds was determined by the balance of the opposing effects: X－H bond lengthening effect due to hyperconjugative $n(Y)\rightarrow\sigma^*(X-H)$ interaction and X－H bond shortening effect due to rehybridization[27]. On the basis of the rehybridization model, the N2－H1…O4 and N5－H6…O3 H－bond formations increase N2－H1 and N5－H6 bond polarization and positive charge on H1 and H6 atom. These changes result in a simultaneous increase in the s-character in the N2 and N5 hybrid orbital of N2－H1 and N5－H6 bonds, which should lead to N2－H1 and N5－H6 bonds contractions. Table 4 shows that the s-character of the N2－H1 bond in the N2－H1…O4 H－bond increases from $sp^{4.03}$ to $sp^{3.79}$ and which strengthens the N2－H1 bond. And the same result is for the N5－H6 bond. In general, the hyperconjugative effect increased the electron density in the $\sigma^*(X-H)$. However, the electron density in the $\sigma^*(X-H)$ decreased instead of increasing. We pay more attention to an interesting phenomenon which is the electron density decreasing in the $\sigma^*(N2-H1)$ and $\sigma^*(N5-H6)$. Hobza showed that reason for the decrease of electron density in $\sigma^*(X-H)$ is electron density redistribution effect[28,29]. On the basis of electron density redistribution effect, we will provide a reasonable model to explain the decrease of electron density in $\sigma^*(X-H)$[30]. In the type Z－X－H…Y H－bond, where Z is an electronegative atom having one or more lone electron pairs (such as F, O, N), the hyperconjugative $n(Y)\rightarrow\sigma^*(X-H)$ interaction leads to an increase of electron density in the $\sigma^*(X-H)$. On the other hand, a decrease in the $n(Z)\rightarrow\sigma^*(X-H)$ interaction of the dimer, relative to the monomer, has the opposite effect. As a result, the net change of electron density in the $\sigma^*(X-H)$ and the ultimate direction of the X－H bond length change depend on the balance of these two interactions which changed in an antiparallel way. It may be of interest to make a quantitative comparison between these two interactions. Then, we define an novel index, called $R_E$, which can be determined as a ratio of the variable magnitude of the $E^{(2)}n(Y)\rightarrow\sigma^*(X-H)$ interaction and the magnitude of the $E^{(2)}n(Z)\rightarrow\sigma^*(X-H)$ interaction in the Z－X－H…Y system. Here, the $R_E$ can be expressed as

$$R_E=\frac{\sum(E^{(2)}[n(Y)\rightarrow\sigma^*(X-H)])}{\sum(E^{(2)}_{\text{monomer}}[n(Z)\rightarrow\sigma^*(X-H)]-E^{(2)}_{\text{dimer}}[n(Z)\rightarrow\sigma^*(X-H)])} \quad (1)$$

Where the $E^{(2)}_{\text{monomer}}[n(Z)\rightarrow\sigma^*(X-H)]$ and $E^{(2)}_{\text{dimer}}[n(Z)\rightarrow\sigma^*(X-H)]$ mean the $n(Z)\rightarrow\sigma^*(X-H)$ interactions in the monomer and the dimer, respectively. The $E^{(2)}[n(Y)\rightarrow\sigma^*(X-H)]$ denotes the $n(Y)\rightarrow\sigma^*(X-H)$ interaction in the dimer. According to the definition of index, the $R_E$ can be used to describe the strength of the electron density redistribution. From the formula, the smaller the value of $R_E$ is, the stronger the electron density redistribution effect is. It can be seen in Table 4 that there a significant decrease of the $E^{(2)}_{n_2(O3)}\rightarrow\sigma^*(N2-H1)$ in the dimer, relative to the monomer HNO. Furthermore, the value of the $R_E$ is 0.5303, which indicates that the electron density redistribution effect is significant in the N2－H1…O4 H－bond of the dimer. Therefore, the electron density in the $\sigma^*(N2-H1)$ and $\sigma^*(N5-H6)$ have an evident decrease can well be interpreted. According to above analysis, the blue shifts of N2－H1 and N5－H6 are attributed to the

Table 5 The differences of R(N－O) and R(N－H) between the dimer and monomer

| | HF/6-311++G(3*df*,3*pd*) | B3LYP/6-311++G(3*df*,3*pd*) | MP2/6-311++G(3*df*,3*pd*) |
|---|---|---|---|
| $\Delta r$(N2－O3)/nm | +0.00028 | +0.00040 | +0.00035 |
| $\Delta r^{CP}$(N2－O3)/nm | +0.00025 | +0.00037 | +0.00026 |
| $\Delta r_1$(N2－H1)/nm | −0.00003 | −0.00008 | −0.00007 |
| $\Delta r_1^{CP}$(N2－H1)/nm | −0.00002 | −0.00007 | −0.00006 |
| $\Delta r_2$(N2－H1)/nm | −0.00030 | −0.00054 | −0.00043 |
| $\Delta r_2^{CP}$(N2－H1)/nm | −0.00028 | −0.00048 | −0.00039 |
| $\Delta v_1/cm^{-1}$ | +68 | 99 | 90 |
| $\Delta v_1^{CP}/cm^{-1}$ | +62 | 90 | 80 |
| $\Delta v_2/cm^{-1}$ | +64 | 89 | 82 |
| $\Delta v_2^{CP}/cm^{-1}$ | +59 | 80 | 73 |
| $\Delta v_{22}/cm^{-1}$ | +6 | +11 | +10 |
| $\Delta v_{22}^{CP}/cm^{-1}$ | +5 | +10 | +8 |

$\Delta r_1$: The differences of N1－H2 distance between the partial optimized monomer and monomer;
$\Delta r_2$: The differences of N1－H2 distance between the dimer and monomer;
$\Delta v_1$: The differences of N1－H2, N5－H6 symmetric stretch between dimer and the monomer;
$\Delta v_2$: The differences of N1－H2, N5－H6 asymmetric stretch between dimer and the monomer;
$\Delta v_{22}$: The differences of N1－H2 stretch between the partial optimized monomer and monomer.

Table 6 The vibrational frequencies of five cycle structure HNO dimer (unit: $cm^{-1}$)

| Methods | Vibrational frequences |
|---|---|
| B3LYP/6-31G* | 28i,103,122,138,206,316,1568,1598,1688,1699,2923,2931 |
| B3LYP/6-311G** | 17i,94,116,164,209,329,1556,1592,1677,1688,2924,2936 |
| B3LYP/6-311+G** | 48i,71,101,155,202,295,1552,1577,1673,1679,2939,2946 |
| B3LYP/aug-cc-pvdz | 38i,68,93,140,187,272,1539,1562,1675,1682,2924,2931 |
| B3LYP/6-311+G(3*df*,2*p*) | 41i,76,93,149,182,277,1552,1573,1675,1681,2936,2945 |
| MP2/6-31G** | 50,107,125,188,206,322,1484,1498,1570,1609,3089,3103 |
| MP2/6-31+G** | 17,78,105,177,205,296.1474,1483,1562,1596,3160,3173 |
| MP2/6-311+G** | 21i,82,101,174,202,277,1496,1507,1568,1599,3091,3115 |
| MP2/aug-cc-pvdz | 11,87,104,161,196,280,1463,1475,1551,1588,3070,3079 |
| MP2/6-311++G** | 26i,82,103,169,201,262,1498,1508,1569,1560,3094,3112 |

rehybridizative effect and electron density redistribution.

### 3.4 Structure reorganization

NBO analysis give the origin of the hydrogen bond blue shift in the electron density transfer way. The structure change effect of HNO in the dimer on the blue shift was discussed in this section. The N－O distances of all optimized dimers are longer than those in the monomers. In order to discuss the N－O elongation effect on the N－H blue shift, the partial optimization on the HNO monomer was performed. The N－O distances of the dimers were remained unchangeable in the optimized processes. The differences of N－H distances between the partial optimized monomer and optimized monomer were listed in the Table 5. From the Table 5, the N－H distances of partial optimized structures are shorter than those of all optimized monomer, which are −0.00003、−0.00008 and −0.00007 nm at HF、B3LYP and MP2 in conjunction with 6－311++G(3df, 3pd) basis set, respectively, which are less than those of N－H distances between dimer and monomer (−0.00030、−0.00054 and −0.00043 nm). Therefore, the N－O elongation is partially contributed to the N－H blue shift. From above analysis, the mechanism for the two blue shift hydrogen bonds is attributed to combination of the three effects: rehybridizative X－H bond strengthening、the electron denisity redistribution X－H

bond strengthening and the structure reorganization effect.

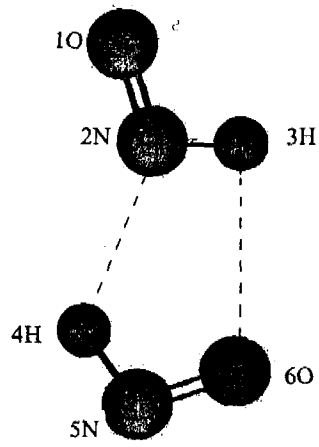


Fig. 2 The five cycle structure for the HNO dimer

## 4 Conclusions

The hydrogen bond interaction of HNO dimer has been analyzed by *ab initio* and density functional theoretical method employing different basis sets levels. N－H···O hydrogen bond stable structure involving the formation is found on the potential energy surface. The dimer exhibits simultaneously contractions of the N2－H1 and N5－H6 and both large blue shifts (about 100 $cm^{-1}$) of $\nu$(N2－H1) and $\nu$(N5－H6) vibrations. From the NBO analysis, it becomes evident that the N2－H1···O4 and N5－H6 ···O3 blue－shifted H－bond, the N2－H1 and N5－H6 bond lengthening effect of hyperconjugation is greatly inhibited due to existence of the significant electron density redistribution effect. Consequently, the N2－H1 and N5－H6 bonds shortening effect is dominant, which leads to a large blue shift of N2－H1 and N5－H6 stretching frequency. Moreover, rehybridizative effect and the structure reorganization are contributed to the large blue shift of the N－H stretching frequency. This work confirmed the truly blue-shifted N－H hydrogen bonds and gave reasonable explanations on the blue-shifted hydrogen bonds. It will be much helpful to understand the nature of the N－H blue shifts in a new way.

**Acknowledgments** This work was supported by the National Natural Science Foundation and Center for Computational Science, Hefei Institutes of Physical Sciences (Grant No. 0330405002).

**References:**

[1] Jeffery G A. An Introduction to Hydrogen Bonding[M]. New York: Oxford University Press, 1997.

[2] Xu B H, Li L C, Tang Z H. Theoretical studies on the interaction between glycine and $H_2O$ [J]. *J. At. Mol. Phys.*, 2003, 20: 275(in Chinese)

[3] Hobza P, Špirko V, Havlas Z, Buchhold K, Reimann B, Barth H－D, Brutschy B. Anti-hydrogen bond between chloroform and fluorobenzene [J]. *Chem. Phys. Lett.*, 1999, 299: 180

[4] Reimann B, Buchhold K, Vaupel S, Brutschy B, Havlas Z, Špirko V, Hobza P. Improper, Blue-shifting hydrogen bond between fluorobenzene and fluoroform [J]. *J. Phys. Chem.*, 2001, A105: 5560

[5] Hobza P, Špirko V, Selzle H L, Schlag E W. Anti-hydrogen bond in the benzene dimer and other carbon proton donor complexes [J]. *J. Phys. Chem.*, 1998, A102: 2501

[6] Hobza P, Havlas Z. Blue-shifting hydrogen bonds [J]. *Chem. Rev.*, 2000, 100: 4253

[7] Gu Y, Kar T, Scheiner S. Fundamental properties of the CH···O interaction: Is it a true hydrogen bond? [J]. *J. Am. Chem. Soc.*, 1999, 121: 9411

[8] Scheiner S, Grabowski S J, Kar T. Influence of hybridization and substitution on the properties of the CH···O hydrogen bond [J]. *J. Phys. Chem.*, 2001, A105: 10607

[9] Scheiner S, Kar T. Red-versus blue-shifting hydrogen bonds: Are there fundamental distinctions? [J]. *J. Phys. Chem.*, 2002, A106: 1784

[10] Matsuura H, Yoshida H, Hieda M, Yamanaka S, Harada T, Shin-ya K, Ohno K. Experimental evidence for intramolecular blue-shifting C－H···O hydrogen bonding by matrix-isolation infrared spectroscopy [J]. *J. Am. Chem. Soc.*, 2003, 125: 13910

[11] Yoshida H, Harada T, Murase T, Ohno K, Matsuura H. Conformational stabilization by intramolecular OH···S and CH···O interactions in 2-(Methylthio) ethanol. Matrix-isolation infrared spectroscopy and *ab Initio* MO calculations [J]. *J. Phys. Chem.*, 1997, A101: 1731

[12] Masunov A, Dannenberg J J, Contreras R H. C－H Bond-shortening upon hydrogen bond formation: Influence of an electric field [J]. *J. Phys. Chem.*, 2001, A105: 4737

[13] Hobza P. N－H···F improper blue-shifting H-bond [J]. *Int. J. Quantum. Chem.*, 2002, 90: 1071

[14] Li X S, Liu L, Schlegel H B. On the physical origin of blue-shifted hydrogen bonds [J]. *J. Am. Chem. Soc.*, 2002, 124: 9639

[15] Lu P, Liu G-Q, Li J-C. Existing problems in theoretical determination of red-shifted or blue-shifted hydrogen bond [J]. *J. Mol. Struct. (Theochem.)*, 2005, 723: 95

[16] Alexander M H, Dagdigian P J, Jacox M E, Colb C E, Melius C F, Rabits J, Smooke M D, Tsang W. Nitramine propellant ignition and combustion research [J]. *Prog. Energy Combust. Sci.*, 1991, 17: 263

[17] Ruud K, Helgaker T, Uggerud E. Mechanism, Energetics and dynamics of a key reaction sequence during the decomposition of nitromethane: HNO + HNO→$N_2O$ + $H_2O$ [J]. *J. Mol. Struct. (Theochem.)*, 1997, 393: 59

[18] Peters N J S. Hydrogen bonding in molecules with more than one proton acceptor site: HOF, HNO, $H_2NF$, and $H_2NOH$ [J]. *J. Phys. Chem.*, 1998, A102: 7001

[19] Boys S F, Bernardi F. The calculation of small molecular interactions by the differences of separate total energies. Some procedures with reduced errors [J]. *Mol. Phys.*, 1970, 100: 65

[20] Reed A E, Curtiss L A, Weinhold F. Intermolecular interactions from a natural bond orbital, donor-acceptor viewpoint [J]. *Chem. Rev.*, 1988, 88: 899

[21] Bader R F W. Atoms in Molecules: A Quantum Theory [M]. Oxford: Oxford University Press, 1990.

[22] Frisch M J, Trucks G W, Schlegel H B, Scuseria G E, Robb M A, Cheeseman J R, Montgomery J A, Jr., Vreven T, Kudin K N, Burant J C, Millam J M, Iyengar S S, Tomasi J, Barone V, Mennucci B, Cossi M, Scalmani G, Rega N, Petersson G A, Nakatsuji H, Hada M, Ehara M, Toyota K, Fukuda R, Hasegawa J, Ishida M, Nakajima T, Honda Y, Kitao O, Nakai H, Klene M, Li X, Knox J E, Hratchian H P, Cross J B, Adamo C, Jaramillo J, Gomperts R, Stratmann R E, Yazyev O, Austin A J, Cammi R, Pomelli C, Ochterski J W, Ayala P Y, Morokuma K, Voth G A, Salvador P, Dannenberg J J, Zakrzewski V G, Dapprich S, Daniels A D, Strain M C, Farkas O, Malick D K, Rabuck A D, Raghavachari K, Foresman J B, Ortiz J V, Cui Q, Baboul A G, Clifford S, Cioslowski J, Stefanov B B, Liu G, Liashenko A, Piskorz P, Komaromi I, Martin R L, Fox D J, Keith T, Al-Laham M A, Peng C Y, Nanayakkara A, Challacombe M, Gill P M W, Johnson B, Chen W, Wong M W, Gonzalez C, and Pople J A. Gaussian 03, Revision B.02, Gaussian, Inc., Pittsburgh PA, 2003.

[23] Hobza P, Havlas Z. Counterpoise-corrected potential energy surfaces of simple H-bonded systems [J]. *Theor. Chem. Acc.*, 1998, 99: 372

[24] Koch U, Popelier P L A. Characterization of C-H-O hydrogen bonds on the basis of the charge denisty [J]. *J. Phys. Chem.*, 1995, 99: 9747

[25] Popelier P L A. Characterization of a dihydrogen bond on the basis of the electron denisty [J]. *J. Phys. Chem.*, 1998, A102: 1873

[26] Lipkowski P, Grabowski S J, Robinson T L, Leszczynski J. Properties of the C-H···H dihydrogen bond: An *ab initio* and topological analysis [J]. *J. Phys. Chem.*, 2004, A108: 10865

[27] Alabugin I V, Manoharan M, Peabody S, Weinhold F. Electronic basis of improper hydrogen bonding: A subtle balance of hyperconjugation and rehybridization [J]. *J. Am. Chem. Soc.*, 2003, 125: 5973

[28] Hobza P, Špirko V. Why is the N1-H stretch vibration frequency of guanine shifted upon dimerization to the red and the amino N-H stretch vibration frequency to the Blue? [J]. *Phys. Chem. Chem. Phys.*, 2003, 5: 1290

[29] Chocholoušová J, Špirko V, Hobza P. First local minimum of the formic acid dimer exhibits simultaneously red-shifted O H···O and improper blue-shifted C H··· O hydrogen bonds [J]. *Phys. Chem. Chem. Phys.*, 2004, 6: 37

[30] Yang Y, Zhang, W J, Pei, S X, Shao J, Huang W, Gao X M. Blue-shifted and red-shifted hydrogen bonds: Theoretical study of the $CH_3CHO$···$NH_3$ complexes [J]. *J. Mol. Struct. (Theochem.)*, 2005, 732: 33